Cyclometalated Rhodium and Iridium Complexes Containing Masked Catecholates: Synthesis, Structure, Electrochemistry, and Luminescence Properties

Antoine Groué, Jean -Philippe Tranchier, Marie Noelle Rager, Geoffrey Gontard, Rémi Métivier, Olivier Buriez, Abderrahim Khatyr, Michael Knorr, Hani Amouri

Cyclometalated Rhodium and Iridium Complexes Containing Masked Catecholates: Synthesis, Structure, Electrochemistry and Luminescent Properties

Antoine Groue, [†] Jean Philippe Tranchier, [†] Marie Noelle Rager,[§] Geoffrey Gontard, [†]Remi Metivier, [#] Olivier Buriez, [‡] Abderrahim Khatyr,[◊] Michael Knorr, [◊] and Hani Amouri*[†]

[†]Sorbonne Université- Campus Pierre et Marie Curie, Institut Parisien de Chimie Moléculaire (IPCM) UMR CNRS 8232, 4 place Jussieu, 75252 Paris cedex 05, France: E-mail: hani.amouri@sorbonne-universite.fr.

[§] Chimie ParisTech, PSL University, NMR Facility, F-75005 Paris, France.

[#] PPSM, ENS Cachan, CNRS, Université Paris-Saclay, 94235 Cachan, France.

[‡] PASTEUR, Département de chimie, École normale supérieure, PSL University, Sorbonne Université, CNRS, 75005 Paris, France.

[◊] Institut UTINAM, UMR CNRS 6213, 16 Route de Gray, Université Bourgogne Franche-Comté, 25030 Besançon, France.

ABSTRACT. Two neutral cyclometalated rhodium and iridium coordination assemblies [(F2ppy)$_2$M(η-Cat)], M = Rh, (**2**); M = Ir (**3**) (F2ppy: 2,4-difluorophenylpyridine) displaying a masked catecholate (η-Cat = η-O^O) are described. The catecholate ligand is π-bonded to the organometallic Cp*Ru(II) moiety. The latter brings stability to the whole system in solution and suppresses the formation of the related paramagnetic semiquinone complex. A determination of the molecular structure of the iridium complex [(F2ppy)$_2$Ir(η-Cat)] (**3**) corroborates the formation of the target compound and reveal the generation of a rare 2D honeycomb supramolecular architecture in the solid state, in which the *Δ*-enantiomer self-assemble with the *Λ-enantiomer* through encoded π-π interactions among individual units. The electrochemistry of complexes **2** and **3** was investigated and showed that reduction occurs at very negative potentials (~ -2.2V vs. SCE), while oxidation of the cyclometalated Rh and Ir centers occur at 0.8 and 0.86 V. In contrast to complexes with 1,2-dioxolene chelates, which are non-emissive, the heterodinuclear diamagnetic complexes **2** and **3** were found to be emissive at room temperature both in solution and in the solid state. Moreover At 77 K in solid state, both compounds display opposite emission behavior, for instance complex **3** displays a blue-shifted emission while the rhodium compound **2** exhibits red-shifted emission to lower energy.

INTRODUCTION

Cyclometalated iridium complexes have received considerable attention because of their important photophysical and electrochemical properties.[1-4] They also show enhanced stability relative to other metal compounds, which make them the adequate complexes to construct stable optical devices in OLEDs technology.[5, 6] The choice of the ancillary ligands plays a crucial role since they bring changes to the photoluminescence quantum yields and also to the emission wavelengths.[1, 7, 8] Moreover, they affect the overall charge of the iridium complexes. Indeed, while neutral cyclometalated iridium(III) compounds are required for OLEDs, cationic species such as [Ir(C^N)$_2$(N^N)]$^+$ with neutral bidentate ancillary ligands have been utilized as light-

emitting-electrochemical cells (LECs).[9] Interestingly the use of 1,2-dioxolene ligands such as benzene-1,2-olate or related aromatic ligands give entrance to a novel class of Ir(III) $[NR_4]$ $[Ir(C\hat{}N)_2(O\hat{}O)]$ salts (Chart 1).[10, 11] The latter have been less investigated compared to the previous classes of iridium compounds, and only few examples have been described in the literature. The reason for this stems from the fact that 1,2-dioxolene chelating ligands are redox active and in solution the *catecholate form* evolves to give the related neutral paramagnetic species in which the1,2-dioxolene ligand adopts the *semiquinone form*.[11, 12] Hence complexes containing 1,2-dioxolene ligands exhibit distinct spectroscopic and absorption properties depending on the ligand upon switching to different oxidation states.[13-15] For example, the anionic iridium salts, which display the catecholate form (Chart 1), are unstable in solution [11], they tend to oxidize towards the more stable neutral species with the *semiquinone* form. Hence, the study of their photophysical properties remains limited.[10]On the other hand the more stable neutral iridium complexes containing the dioxolene ligand in the *semiquinone form* (Chart 1) are non-luminescent as demonstrated by *Thompson et al.*.[12]

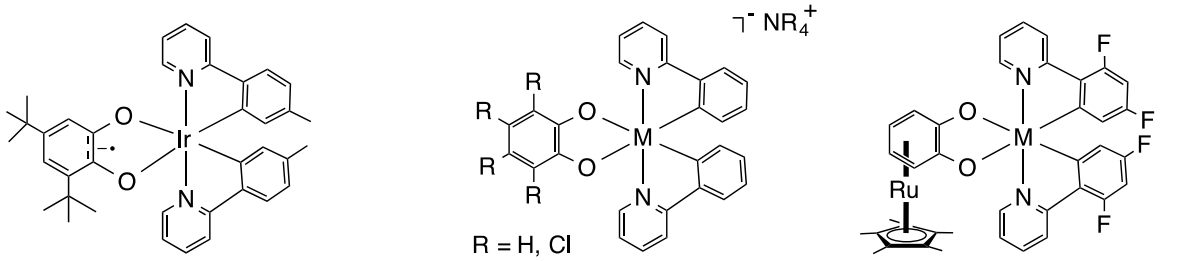

Thompson et al. *Inorg. Chem.* 2007 | Szerb et al. *Inorg. Chem. Comm.* 2013 Housecroft, Constable et al. *Polyhedron* 2016 | M = Rh (**2**) ; M = Ir (**3**), this work

Chart 1.

In a previous work, we demonstrated that organometallic scaffolds of the type "Cp*M, M = Ru, Rh and Ir" are able to stabilize reactive intermediates by changing their electronic properties.[16] For instance, π-bonded quinonoid complexes such as $[Cp^*M(o\text{-}C_6H_4O_2)]^n$, where M = Ru, n = -1; M = Rh, Ir, n = 0, Cp* = pentamethylcyclopentadienyl.[17, 18] We also isolated and described the analogous thio- and seleno-quinonoid compounds.[19, 20] In fact due to their O, S, Se donor atoms, these quinonoid compounds are employed as organometallic-ligands "OM-ligands" to design

novel type of phosphorescent supramolecular assemblies. Noteworthy, the presence of Cp*M renders these OM-ligands more electron-donor "*i.e.* a masked catecholate ligand (η-Cat)" and enhances the solubility of the obtained coordination compounds.[21, 22]

Thus using our approach, we prepared novel type of phosphorescent $[M(N^N)_2(\eta\text{-Cat})]^{2+}$ compounds (Cat = η-O^O). The presence of a Cp*Ru moiety in the organometallic ligand permits to tune the electronic properties of such molecules, affording compounds capable to absorb along the whole range of the visible spectrum and displaying interesting luminescent properties.[23-29] Therefore, these metallo-ligands play an important role in the design of novel class of $[(\eta\text{-O^O})Ru(N^N)_2]^{2+}$ complexes featuring new properties. Thus, we envisioned preparing a novel class of luminescent cyclometalated rhodium and iridium complexes containing π-bonded dioxolene ligands. The latter acts as masked catecholate. In this work, we describe the synthesis and luminescent properties of some heterobimetallic cyclometalated compounds containing masked *catecholate ligands* (Figure 1). Our synthetic approach provides neutral stable catecholates **2** and **3** forming in the solid state original network architectures and are exhibiting interesting electrochemical and photophysical properties.

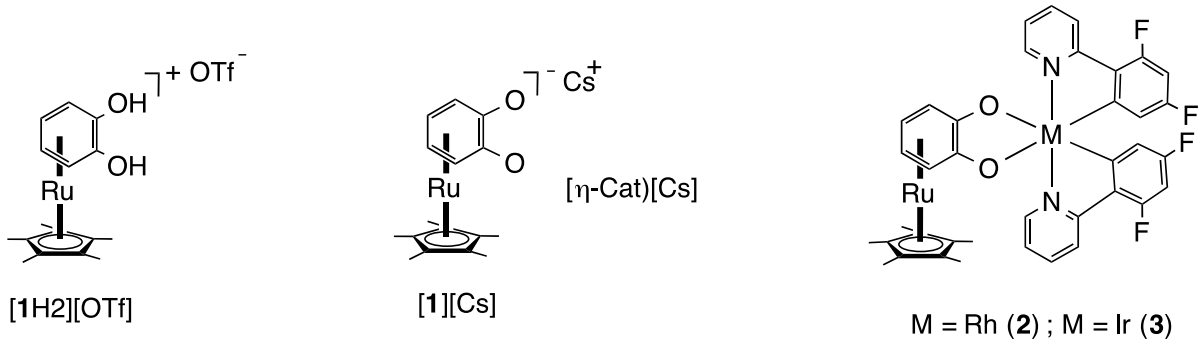

Figure 1. Schematic drawing of the catechol ruthenium complex [**1**H2][OTf], the masked catecholate ligand [**1**][Cs] and the target compounds $[(F2ppy)_2M(\eta\text{-Cat})]$ (**2**-**3**).

RESULTS and DISCUSSION

*Synthesis of the cyclometalated rhodium and iridium assemblies [(F2ppy)$_2$M(η-Cat))] (**2-3**) with masked catecholate ruthenium units*.

The dinuclear coordination assemblies [(F2ppy)$_2$Rh(η-Cat] (**2**) and [(F2ppy)$_2$Ir(η-Cat] (**3**) were obtained in two reaction steps. The first step consists of treating the halogenated precursor [M(F2ppy)$_2$(μ-Cl]$_2$ with silver triflate salt in acetone at ambient temperature to generate the solvated cyclometalated salt complexes [(F2ppy)$_2$M(solvent)$_2$][OTf] (Scheme 1). Subsequently the solvated species is treated with [Cp*Ru(*o*-C$_6$H$_4$O$_2$][Cs] [**1**][Cs] for one hour. After work-up, the desired compounds [(F2ppy)$_2$Rh(η-Cat)] (**2**) and [(F2ppy)$_2$Ir(η-Cat)] (**3**) have been isolated as dark purple and green air stable microcrystalline solids in 47% and 67% yields.

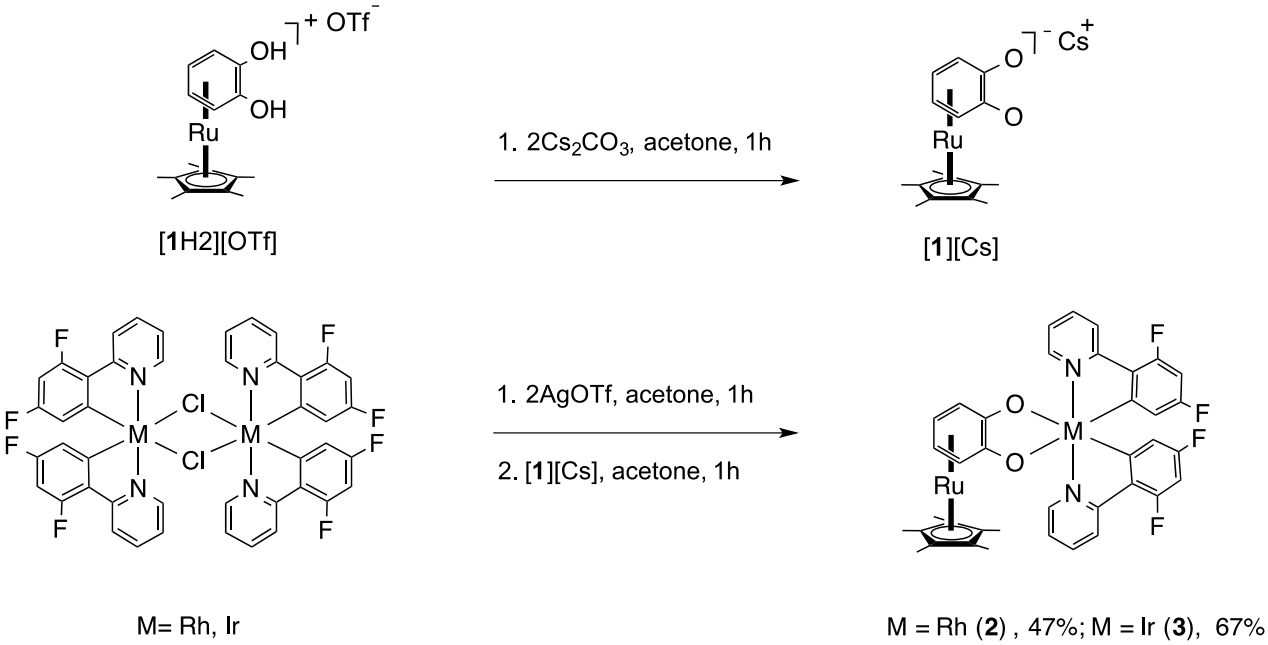

Scheme 1. Synthesis of the cyclometalated rhodium and iridium complexes **2-3**.

The heteronuclear assemblies [(F2ppy)$_2$M(η-Cat] M = Rh, (**2**); M = Ir, (**3**) were completely identified by ^{1}H- and ^{13}C-NMR NMR spectroscopic techniques and microanalysis, furthermore the solid-state structure was ascertained by single crystal x-ray diffraction study. For example, the ^{1}H-NMR spectrum of [(F2ppy)$_2$Rh(η-Cat)] (**2**) recorded in CD_2Cl_2 showed

multiple resonances indicating a lack of symmetry in these compounds as expected. Indeed, we note the presence of 12 peaks attributed to the "ppy moiety" which are visible at δ 5.4-9.1 ppm. Moreover, the ^{1}H-resonances of the η-catecholate appear as four multiplets at δ 4.4-5.0 ppm due to the lack of symmetry. Finally, ^{1}H-resonances of the C_5Me_5Ru give rise to a singlet at δ 1.70 ppm. Complete characterizations of **2-3** are presented in the experimental part.

*Molecular structure of the Cyclometalated iridium complex **3** and formation of a 2D honeycomb supramolecular architecture*.

After many attempts, X-ray suitable yellowish-green crystals of **3** crystallizing in the triclinic space group P1 were obtained by slow evaporation of hexane into a saturated THF solution of **3**. The asymmetric unit contains two independent molecules. The molecular structure of **3** is depicted in Figure 2. The structure shows the mode of coordination of the masked catecholate ligand **1** in which the O^O chelates to the $Ir(F2ppy)_2$ moiety via the two oxygen atoms. The structure shows also, the Ir(III) is coordinated to two F2ppy units. As expected the metalated carbon centers are disposed in *cis*-geometry while the nitrogen centers are arranged in a *trans*-configuration, confirming the formation of the target molecule $(\eta\text{-O^O})Ir(F2ppy)_2$. Consequently, the metal center is bound to three chelating ligands imposing a distorted octahedral geometry. The average Ir-N and Ir-C bond distances are of 2.03(1) Å and 1.99(1) Å in line with those results obtained for similar compounds.[21, 23-25, 30] The six-membered carbocycle ring is bound to the Cp*Ru fragment in a η^6-mode, the mean Ru-C bond distance is 2.22(3) Å for the internal diene system (C25 and C28) and 2.40(6) Å for C23 and C24, slightly longer but also indicative of a bonding interaction. Moreover, the mean C-O bond length is 1.31(2) Å, in accord of a single bond. The hinge angle, across C25—C28, is 6.4(10)° reflecting a slight deviation from planarity. In summary, the solid-state structure of $[(F2ppy)_2Ir(\eta\text{-Cat}]$ **(3)** demonstrates that the η-O^O chelating ligand adopts a *catecholate* form.

An examination of the packing of complex **3** in the crystal structure reveals the generation of a 2D honeycomb architecture. The latter is made of single molecules that are encoded through π-π interactions from several units, namely (i) between the phenyl rings of two adjacent F2bpy units (*circa* 3.39 Å), and (*ii*) between two pyridine rings of two adjacent F2bpy units (*circa* 3.30 Å) and between two Cp*Ru units of two adjacent molecules (*circa* 3.73 Å). These π-π interactions occurred among six adjacent molecules in two different directions and generate the honeycomb supramolecular structure (see Figure 2b).

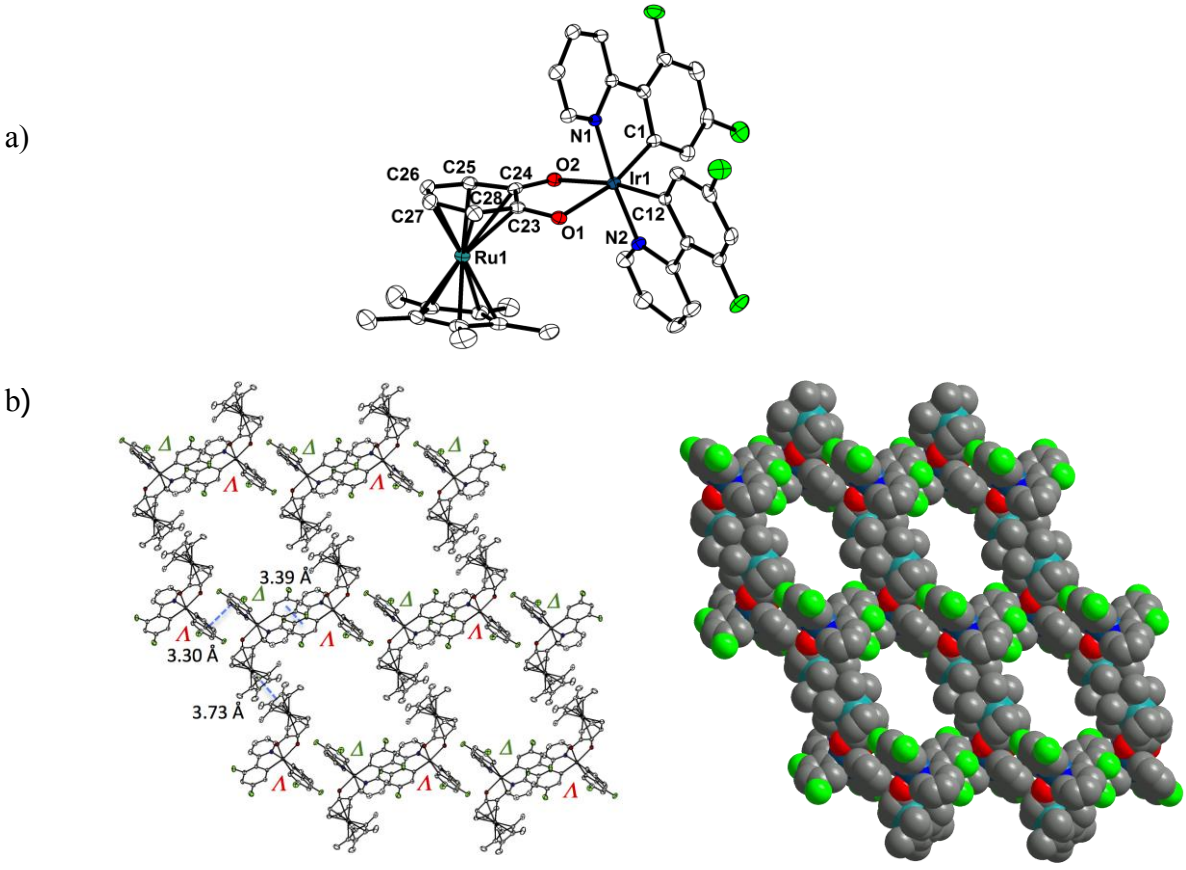

Figure 2. a) Molecular structure of [(F2ppy)$_2$Ir(η-Cat] **(3)** with partial atom numbering scheme. b) Solid-state arrangement among individual molecules through π-π contacts giving rise to a 2D honeycomb supramolecular architecture.

*Solution behavior and resolution of complex **3** into distinct single enantiomers.*

To examine whether this supramolecular architecture is maintained in solution or whether aggregates may form among individual units we recorded the ^{1}H DOSY spectrum of **3** and measured the diffusion coefficient of **3** in CD_2Cl_2 (See Figure S3).

The diffusion coefficient for complex **3** was found to be $1.34 \pm 0.03\ 10^{-9}$ m^2 s^{-1}, and close to that of the rhodium complex **2** with $D = 1.45 \pm 0.02\ 10^{-9}$ m^2 s^{-1} (Figure S2). For comparison purposes, the diffusion coefficient of the starting material Ir(F2ppy)$_2$(μ-Cl]$_2$ was estimated to be $8.00 \pm 0.01\ 10^{-10}$ m^2 s^{-1} (Figure S1). These findings suggest that in solution, both compounds do not form aggregates and exclude the hypothesis that the supramolecular assembly of **3** is maintained in solution. Despite several attempts, we failed growing single-crystals of the enantiopure complex **3** in order to examine its arrangement in the solid state and comparing it to that of the racemic compound **3**.

Thus *rac*-[Ir(F2ppy)$_2$(μ-Cl]$_2$ was first resolved by treatment with either *L*-proline or *D*-proline and following the experimental procedure described in the literature for *rac*-[Ir(ppy)$_2$(μ-Cl]$_2$.[31-33] We note however that other methods have been employed to resolve such complexes displaying chiral at metal center.[34-36] In a second step the single diastereomer whether *Δ*-[Ir(F2ppy)$_2$(*D*-pro)] (*Δ*-**4**) or *Λ*-[Ir(F2ppy)$_2$(*L*-pro)] (*Λ*-**4**) was treated with TFA in CH_3CN to remove the chiral auxiliary subsequent treatment with the organometallic ligand [Cp*Ru(*o*-$C_6H_4O_2$][Cs] ([**1**][Cs]) in acetone provided the target enantiopure compounds *Δ*-[(F2ppy)$_2$Ir(η-Cat)] (*Δ*-**3**) and *Λ*-[(F2ppy)$_2$Ir(η-Cat)] (*Λ*-**3**) in 14% and 21% yields respectively (See experimental section). The ^{1}H-NMR spectra recorded in CD_2Cl_2 confirmed the purity of the compounds. Moreover, the CD traces of *Δ*-[(F2ppy)$_2$Ir(η-Cat)] (*Δ*-**3**) and *Λ*-[(F2ppy)$_2$Ir(η-Cat)] (*Λ*-**3**) recorded in CH_2Cl_2 showed a mirror image underpinning the relationship between the two enantiomers (Figure 3).

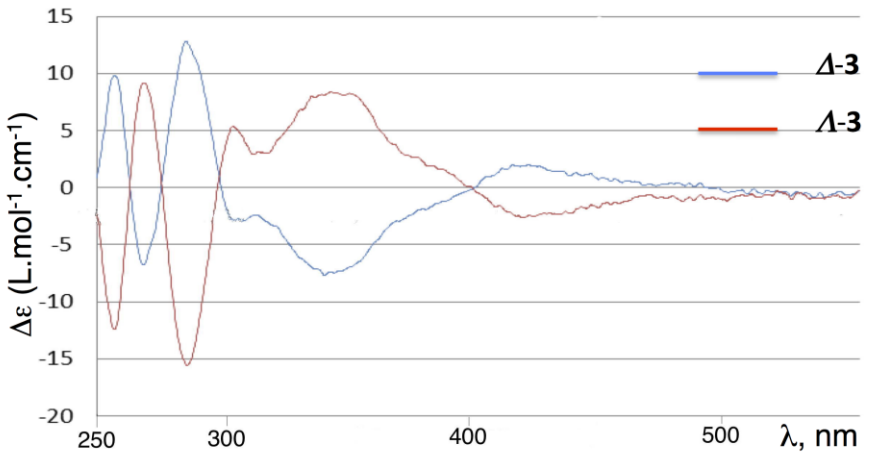

Figure 3. CD traces of *Λ*-**3** (red line) and *Δ*-**3** (blue line) showing mirror image. Recorded in CH_2Cl_2 at C = 0.2 mM.

Unfortunately, all our attempts to grow suitable crystals of either optically active complex *Λ*-**3** or *Δ*-**3** were unsuccessful. Although the main purpose of this work is not the investigation of the optical properties of enantiopure materials, yet our method might serve as a valuable tool for those who are interested in the resolution of chiral complexes into their corresponding enantiomers.[37-39]

Electrochemistry of the Cyclometalated rhodium and iridium complexes ***2-3***

Redox properties of complexes **2** and **3** were investigated by cyclic voltammetry. Experiments were performed, under argon and at room temperature, in dichloromethane containing a supporting electrolyte ($n$$Bu_4NBF_4$ at a concentration of 0.3 M). The working (0.5 mm in diameter) and counter (1 cm in length) electrodes were in platinum. Potential values were measured versus a Saturated Calomel Electrode (SCE). In Table 1 are gathered the oxidation and reduction peak potential values measured for complexes **2** and **3**. The cyclic voltammogram of **3** showed a first oxidation wave, which is reversible at high scan rates (e.g. $50V.s^{-1}$ as shown in Figure 4(b)). Under the same conditions, a second oxidation process was also observed at a more positive potential value, but its reversibility was not as clearly defined as for the previous one. By analogy with reported works on similar complexes these two successive oxidation processes can be assigned to the Ir^{III}/Ir^{IV} and Ru^{II}/Ru^{III} redox couples, respectively.[25, 29, 40]

Compared to iridium complex **3**, the rhodium analogue **2** exhibits a first process which is reversible at low scan rates (e.g. 0.1V/s) showing that replacing the Ir atom metal center with a Rh one leads to a more stable oxidized species (compare Figures 4(b) and 5(b)). This process can be assigned to the Rh^{III}/Rh^{IV} redox couple. Nevertheless, under the same conditions (scan rates, electrode, solvent…) the second oxidation process corresponding to the Ru^{II}/Ru^{III} redox couple could not be evidenced.

Scanning in the cathodic region resulted in an ill-defined reduction wave at around -2.15 / -2.20 V for both complexes **2** and **3** (Figures 4(a) and 5(a)). By comparison with a recent work on the $[Ir(F2ppy)_2(C\hat{}C)]$ complexes[41], this process which was visible only at slow scan rates (0.1V/s typically), due to a too slow electron transfer rate, can be assigned to the reduction of the 2-(2,4-difluorophenyl)pyridine ligand.

The energy gap ΔE(HOMO-LUMO) that corresponds to the electronic transition of lower energy, could be evaluated by determining the potential gap between the first oxidation potential and the first reduction potential *i.e.*, $|E^{p}_{red} - E^{\circ}_{ox}|$. Note that the value of E^{p}_{red} (p for peak potential) was used instead of E°_{red} because the latter could not be obtained as a consequence of the nonreversible nature of the reduction process. Accordingly, a value close to 3 V was found for each complex (3.06 and 2.95 V for complex **3** and **2**, respectively).

Complex	**Oxidation Peak Potential**	**Reduction Peak Potential**
3 (Ir/Ru)	a) E°_{ox} = + 0.86 [a] b) E^{p}_{ox} = + 1.43 [a]	E^{p}_{red} = -2.20 [b]
2 (Rh/Ru)	a) E°_{ox} = + 0.80 [b] b) not visible	E^{p}_{red} = -2.15 [b]

Table 1: Redox properties of complexes **2** and **3**. All potentials were performed at a platinum disk electrode (0.5 mm in diameter). Complexes were dissolved, at room temperature, in CH_2Cl_2 (2 mM) in presence of nBu$_4$NBF$_4$ (0.3 M) as the supporting electrolyte. E^{p}_{red}: reduction peak potential. E^{p}_{ox}:oxidation peak potential. E°_{ox}: standard potential. [a] at a scan rate of 50 V/s. [b] at a scan rate of 0.1 V/s.

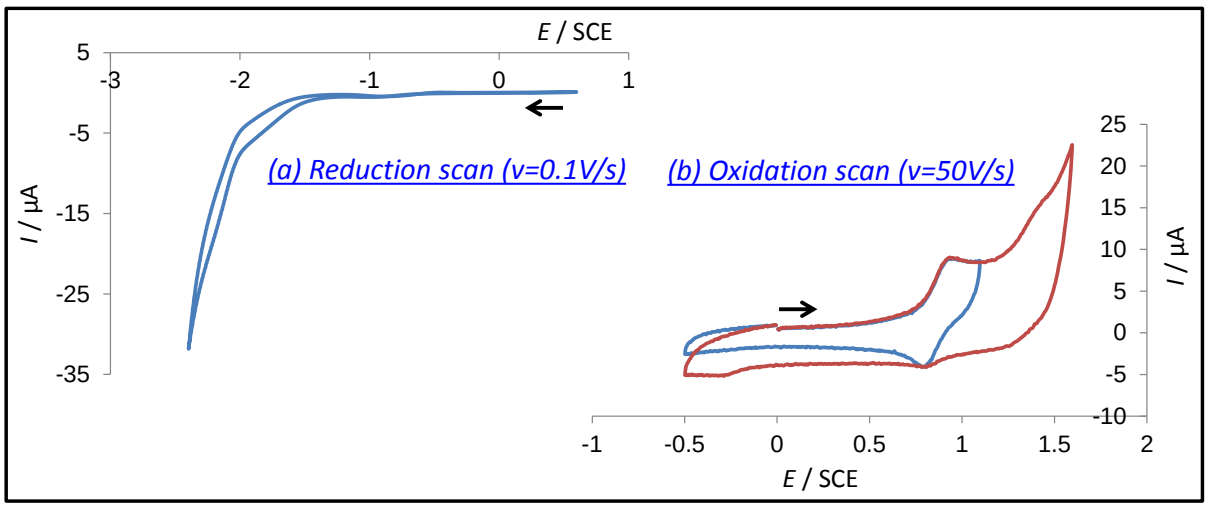

Figure 4. Cyclic voltammetry of complex **3** (2 mM) in CH_2Cl_2 in presence of nBu$_4$NBF$_4$ (0.3M) at a platinum disk electrode (0.5 mm in diameter). (a) Cathodic scan at 0.1 V.s^{-1}and (b) anodic scan at 50 V.s^{-1}.

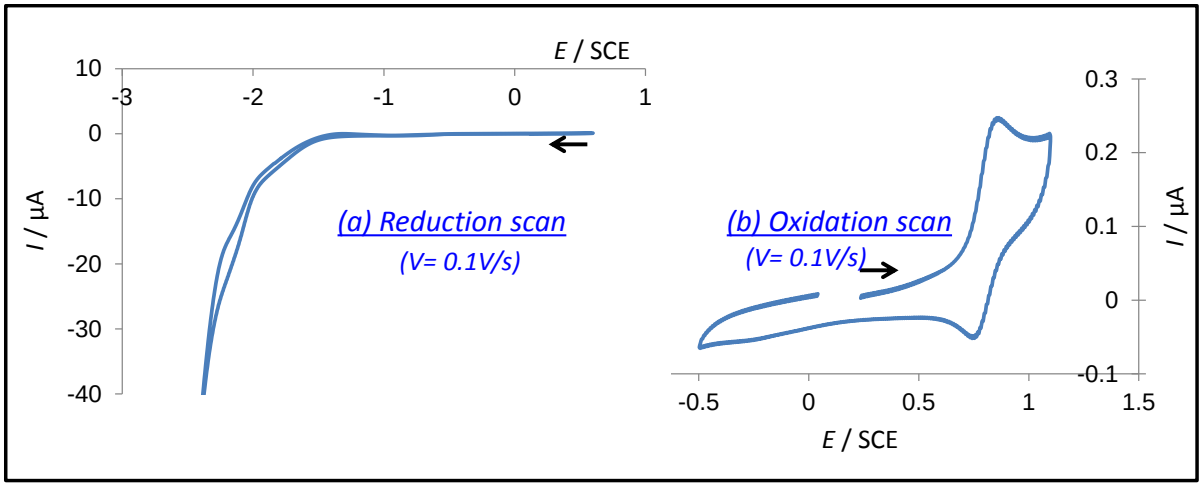

Figure 5. Cyclic voltammetry of complex **2** (2 mM) in CH_2Cl_2 in presence of nBu$_4$NBF$_4$ (0.3M) at a platinum disk electrode (0.5 mm in diameter) and at a scan rate of 0.1 V.s^{-1}. (a) Cathodic scan and (b) anodic scan.

*Absorptions and emissions of **2** and **3**.*

Complexes **2-3** were dissolved CH_2Cl_2 and their absorption spectra were investigated (Figure 6). The absorption parameters are given in Table 2.

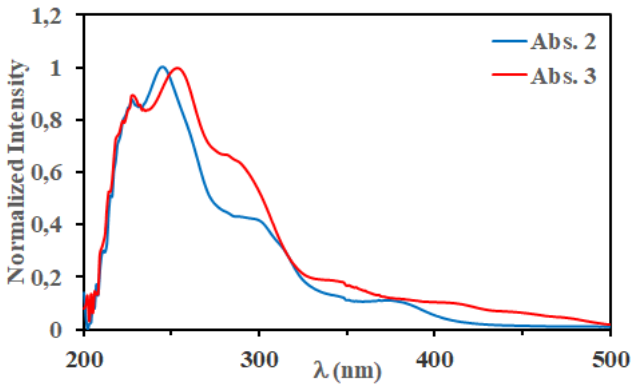

Figure 6. Absorption spectra of **2** (blue) and **3** (red) recorded in CH_2Cl_2 solution at room temperature.

The heterodinuclear compounds **2-3** exhibit a comparable high-energy absorption profile centered at 260−280 nm. This transition can be assigned to a spin-allowed $^1\pi,\pi^*$ ligand-centered (^{1}LC) transitions of the difluorophenylpyridine ligands, with probably some contribution from ^{3}LC forbidden transitions,[1, 42] due to the presence of the heavy-atom such as iridium and rhodium nuclei (ζ_{Rh} = 1259 cm^{-1}; ζ_{Ir} = 3909 cm^{-1}). [43] Moreover we notice the presence of low intensity bands at 370 nm for complex **2** and a large band that tails up to 500 nm for **3** ($\varepsilon < 10^4$ M^{-1}·cm^{-1}), This bands might be tentatively assigned as admixture of ^{1}MLCT transitions related to the M(F_2ppy) (M = Rh, Ir) moieties and to charge transfer transitions from the occupied d metal orbitals to the π* molecular orbitals of the π-bonded catecholate moiety, either of σ-bond to ligand charge transfer (^{1}SBLCT) or mixed ^{1}MLCT/ ^{1}ILCT character. Previously, we investigated by TD-DFT calculations the electronic properties of such complexes displaying Ru(II)-catecholate ligands (η-Cat). The calculations demonstrated that (η-Cat) ligand affects strongly the highest occupied MOs (HOMOs).[24] Moreover these studies showed that, the low energy LUMOs are mostly located on the "ppy" moieties.

Table 2. Absorption parameters [a]

	λ_{max}, nm ($\varepsilon_{max} \times 10^{-3}$, $M^{-1} \cdot cm^{-1}$)
2	227 (37.7), 245 (42.9), 300 (17.9), 375 (4.6)
3	228 (35.4), 254 (39.3), 290 sh (24.7), 413 (3.8)

[a] Recorded in dichloromethane at ambient temperature.

At room temperature in CH_2Cl_2 solution, the rhodium and iridium complexes **2** and **3** were found to be luminescent. For instance, the rhodium complex [(F2ppy)$_2$Rh(η-Cat] (**2**) displays vibronic emission bands at λ = 378 nm, 399 nm, 419 nm (sh) with $\phi = 9x10^{-4}$, the life-time τ = 11.68 ns suggesting that the emissions might originate from ^{3}LLCT transitions.[42, 44, 45] The vibrational progressive spacing for complex **2** was estimated to be 1393 cm^{-1}, indicating that the skeletal vibration can be assigned to the cyclometalated phenyl pyridine ligand. The iridium complex [(F2ppy)$_2$Ir(η-Cat] (**3**) exhibits rather a broad emission band at λ_{max} = 475 nm with $\phi = 4.3x10^{-3}$ τ = 38.75 ns, which might originate from a ^{3}LC-^{3}MCLT transitions (Figure 7).[46] For comparison purposes with respect to a previous work on related [(MEppy)$_2$M(η-Cat)] (ME = methylester; M = Rh, Ir) [30] but containing an ester group at the pyridyl unit instead of the phenyl ring, we studied the luminescent properties of both compounds **2**-**3** in MeOH/EtOH (1/4) mixture at room temperature and at 77 K. Unlike the iridium ester compound, which emits in the red region (λ_{max} = 600 nm), our current compounds displayed emissions at higher energy (vide infra). It should be mentioned that the rhodium ester compound is not emissive. In contrast and interestingly, the rhodium complex [(F2ppy)$_2$Rh(η-Cat)] (**2**) displays vibronic bands emission at λ = 375 nm, 396 nm, 416 nm (sh) similar to those displayed in dichloromethane solution. At 77 K the vibronic bands pattern evolve, thus in addition to those displayed at room temperature, we notice that novel bands red shifted appear at λ = 445 nm and at λ = 476 nm. As for the iridium complex [(F2ppy)$_2$Ir(η-Cat] (**3**), the normalized emission spectrum at room temperature displays a broad band at λ_{max} = 508 nm. At 77K a more structured emission band is seen with λ_{max} = 489 nm. This

emission is blue-shifted relative to that displayed at room temperature (Figure S4). The relevant photophysical data are shown in Table 3. The presence of the fluorine substituents at the cyclometalated ring (F2ppy) should stabilize the HOMO level and hence enlarges the HOMO-LUMO gap in these compounds **2-3** when compared to the $[(MEppy)_2M(\eta\text{-Cat})]$ species.

Table 3. Emission parameters for complexes **2-3**

	298 K [a]					77 K [b]
	λ, nm	ϕ (%)	τ, ns	k_r, s^{-1}	k_{nr}, s^{-1}	λ, nm
2	378, 399, 419(sh)	$9x\ 10^{-4}$	11.68	$7.7x\ 10^4$	$8.6\ x\ 10^7$	374, 385, 395, 415, 445, 476 (sh)
3	384, 403, 449(sh), 475, 505(sh),	$4.3\ x\ 10^{-3}$	38.75	$58.6\ x\ 10^4$	$13.6\ x\ 10^7$	489, 523 (sh)

a. Recorded in CH_2Cl_2. b. Recorded in MeOH/EtOH(1/ 4)

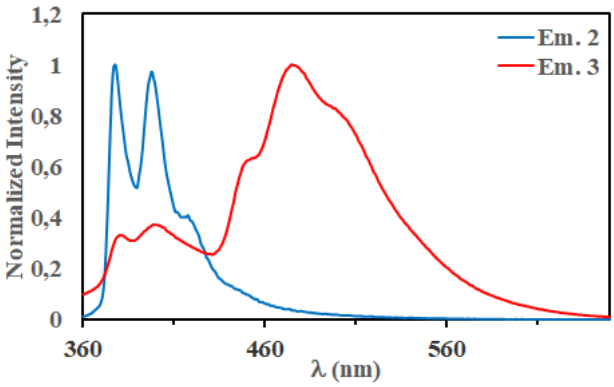

Figure 7. Emission bands of **2** (blue) and **3** (red) recorded in CH_2Cl_2 at ambient temperature.

Moreover, complexes **2** and **3** were also found to be emissive in condensed media at ambient temperature. For example, the rhodium compound **2** displays a less structured emission at λ_{max} = 450 nm when compared to that observed in CH_2Cl_2 solution. The iridium complex **3** exhibits a broad band at λ = 532 nm. Upon cooling, the samples at 77K the iridium compound displayed a slightly blue shifted emission at λ = 527 nm. In contrast, the rhodium complex **2** displays a broader band at λ = 427 nm, we also note in Figure 8, the appearance of at least two novel red-

shifted broad bands at λ = 525 nm and approximately at λ = 676 nm due to the measure limitations of our spectrophotometer.

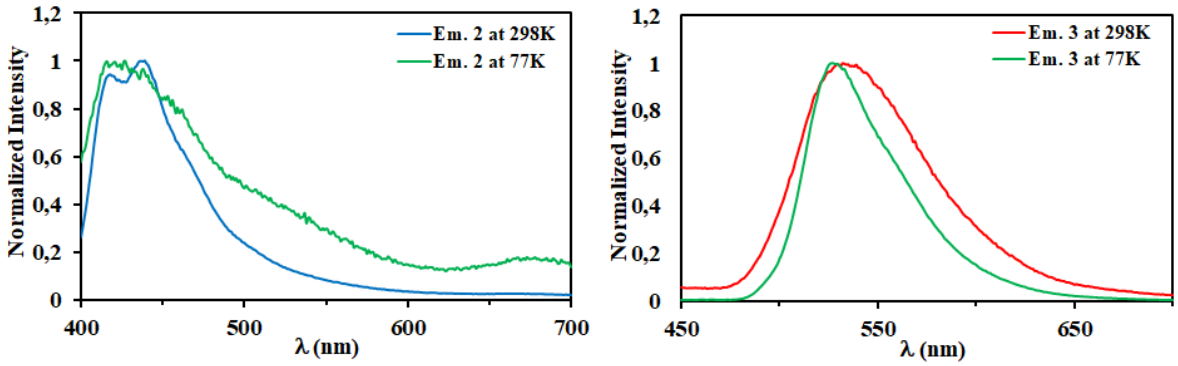

Figure 8. Emission spectra of complexes **2** (left) and **3** (right) recorded in solid state at 298K and 77K.

At this stage, a comment on the low temperature emissions behavior for complexes **2** and **3** is required. The data obtained at low temperature for **2** suggests a completely different behavior when compared to the iridium complex **3**. For instance, the latter behaves as a single species whether in solution or in solid state (at supramolecular level). In contrast, the rhodium compound **2**, appears to display stronger π-π interactions among individual units which at supramolecular level or condensed media affect dramatically the emissions at low temperature and novel low-energy bands in the red and even in the NIR regions. This behavior is rather interesting and illustrates a nice example of structure-property relationship, which could be useful for future applications as luminescent devices.

Conclusions

We have synthesized and fully characterized two stable complexes $[(F2ppy)_2M(\eta\text{-Cat}]$ M = Rh, **(2)**; M = Ir **(3)** bearing masked π-bonded catecholates. A determination of the crystal structure of the iridium species $[(F2ppy)_2Ir(\eta\text{-Cat}]$ reveals the occurrence of several π-π interactions between individual units generating a 2D honey-comb supramolecular architecture the solid-state. The ^{1}H DOSY studies in solution at room temperature were carried out on **2** and **3** to see whether these interactions are maintained in solution. On the other hand compound **3**

was resolved using a chiral auxiliary procedure. The CD traces of both enantiomers *Δ*-[(F2ppy)$_2$Ir(η-Cat)] (*Δ*-**3**) and *Λ*-[(F2ppy)$_2$Ir(η-Cat)] (*Λ*-**3**) were recorded in CH_2Cl_2 and confirmed the presence the enantiomeric relationship between both compounds. The electrochemistry of complexes **2** and **3** were investigated and showed that reduction occurs at very negative potentials (~ -2.2V) while oxidation of the cyclometalated Rh and Ir centers occur at 0.8 and 0.86 V. Thus the redox gap is large around 3V when compared the related ruthenium complexes.[25]

Moreover, the photophysical properties of both compounds [(F2ppy)$_2$Rh(η-Cat] (**2)** and [(F2ppy)$_2$Ir(η-Cat] (**3**) have been studied in solution and in solid state at ambient temperature and at low temperature, showing that these compounds are luminescent. This contrast to related compounds displaying 1,2 dioxolene, which are non-luminescent and relatively unstable. At 77 K in condensed media the rhodium and the iridium complexes displayed an opposite behavior. For instance, while complex **3** behaved as a single species in solution and in condensed media, in contrast the rhodium compound **2** in solid state and at low temperature, displayed novel emission bands in the red and NIR regions reminiscent of π-π interactions among individual units at supramolecular level in the excited state. This result illustrates an interesting example of structure-property relationship for future applications as smart optical devices.

AUTHOR INFORMATION

Corresponding Author

*E-mail: hani.amouri@sorbonne-universite.fr.

Author Contributions

The manuscript was written through contributions of all authors. All authors have given approval to the final version of the manuscript.

Funding Sources

ACKNOWLEDGMENTS

This work was supported by the CNRS, by the Sorbonne Université, which we gratefully acknowledged. M. N. R. acknowledges support from Ile de France Region for funding a 500 MHz NMR spectrometer of Chimie-ParisTech in the framework of the SESAME equipment project (n°16016326).

Experimental Section

Apart from the chlorides/anions metathesis workup, which has been performed under air, all other experimental manipulations were carried out under argon atmosphere using Schlenk tube techniques. Standard techniques were used for the solvents purification. A Bruker Avance 300 NMR or Avance NEO 500 spectrometer was used for recording the ^{1}H NMR and ^{13}C NMR spectra in CD_2Cl_2. For the UV-Vis spectra, a VARIAN-Cary 300 array spectrophotometer was used. A Jobin-Yvon Fluoro Log 3 spectrofluorometer equipped with a R928P detector was employed for recording the steady state excitation and emission spectra both in the solid state (298 K and 77 K) and in solution at room at ambient temperature.

$[Ru(bpy)_3]Cl_2$ ($Ø_L$ = 0.028) served as luminescence quantum yield standard for the determination of the luminescence quantum yields $Ø_L$ at 298 K.[31] For the solid-state photophysical studies, a quartz tube inside a quartz-walled Dewar flask was filled with the solid samples. In a similar manner, an optical Dewar flask filled with liquid N_2 was used for the measurements of the solid-state samples at 77 K. Spectrophotometric-grade dry dichloromethane was used for the photophysical studies in solution. A FL-R928P-TCSPC apparatus equipped with a DeltaDiode source was used for recording the luminescence decay signals. The Decay Analysis Software DAS6 was employed for the analysis of the luminescence decay profiles against time.

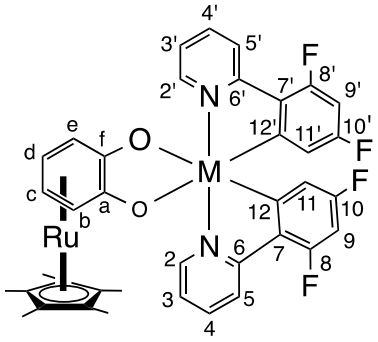

Synthesis of [(F2ppy)$_2$Rh(η-Cat)] (2)

After dissolution of $[(F2ppy)_2Rh(\mu\text{-}Cl)]_2$ (160 mg, 0.16 mmol) at room temperature in acetone solution (5 ml), two equivalents of AgOTf (84 mg, 0.32 mmol) were added. After 20 min, precipitation of AgCl was noticed and the solution turned to yellowish and stirring was continued for one hour. In parallel, a solution of [Cp*Ru(η-catechol][OTf] (160 mg, 0.32 mmol) in acetone (5 ml) was prepared in a second Schlenk tube and two equivalents of Cs_2CO_3 (215 mg, 0.64 mmol) were added in one portion. After stirring for one hour to generate *in situ* the [Cs][η-Cat)] salt, a filtered yellow solution of $[(ppy)_2Rh(solvent)_2]^+$ was mixed with the [Cs][η-Cat)] suspension. After stirring for an additional hour and subsequent removal of the solvent under vacuum, the residue was extracted with dichloromethane and filtered through celite. Evaporation of CH_2Cl_2 under vacuum provided the bimetallic complex as purple solid (130 mg, 46% yield). ^{1}H NMR (500 MHz, CD_2Cl_2), δ (ppm) 9.07 (dd, J = 5.8; 0.8 Hz, 1H, H_2), 8.66 (dd, J = 5.8; 0.8 Hz, 1H, $H_{2'}$), 8.25 (d, J = 8.3 Hz, 1H, H_5), 8.16 (d, J = 8.2 Hz, 1H, $H_{5'}$), 8.00 - 7.96 (m, 1H, H_4), 7.83 – 7.80 (m, 1H, $H_{4'}$), 7.44 (ddd, J = 7.2; 5.8; 1.3 Hz, 1H, H_3), 7.17 (ddd, J = 7.2; 5.8; 1.3 Hz, 1H, $H_{3'}$), 6.43 – 6.36 (m, 1H, H_9), 6.39 – 6.33 (m, 1H, $H_{9'}$), 5.69 - 5.66 (m, 1H, H_{11}), 5.50 - 5.47 (m, 1H, $H_{11'}$), 4.96 (dd, J = 5.6; 1.1 Hz, 1H, H_e), 4.86 (dd, J = 5.6; 1.1, 1H, H_b), 4.47 (ddd, J = 5.6; 5.0; 1.1 Hz, 1H, H_c), 4.42 (ddd, J = 5.6; 5.0; 1.1 Hz, 1H, H_d), 1.70 (s, 15H, H-Cp*). ^{13}C NMR (125 MHz, CD_2Cl_2) δ 173.4 (broad d, J_{CRh} = 34.0 Hz, C_{12}), 172.9 (broad d, J_{CRh} = 35.0 Hz, C_{12}), 162.2 (d, J_{CF} = 7.3 Hz, C_6), 162.1 (d, J_{CF} = 7.3 Hz, $C_{6'}$), 161.7 (dd, J_{CF} = 256.0; 12.0 Hz, C_{10}), 161.6 (dd, J_{CF} = 256.0; 12.0 Hz, $C_{10'}$), 160.1 (dd, J_{CF} = 260.0; 13.0 Hz, $C_{8'}$), 160.0 (dd, J_{CF} = 260.0; 13.0 Hz, C_8), 150.4 (C_2), 149.0 ($C_{2'}$), 148.0 (C_a), 142.1 (C_f), 137.7 (C_4), 137.6 ($C_{4'}$), 127.8 (t, J_{CF} = 3.2 Hz, $C_{7'}$), 127.7 (dd, J_{CF} = 4.6; 2.8 Hz, C_7), 122.7 (d, J_{CF} = 19.0 Hz, C_5 and $C_{5'}$), 122.3 (C_3), 122.0 ($C_{3'}$), 115.5 (dd, J_{CF} = 17.4; 2.8 Hz, C_{11}), 114.8 (dd, J_{CF} = 17.4; 2.8 Hz, $C_{11'}$), 98.0 (t, J_{CF} = 26.8 Hz, C_9, $C_{9'}$), 88.9 (Cq-Cp*), 78.5 (C_e), 76.7 (C_d), 76.5 (C_c), 75.6 (C_b), 10.4 (CH_3-Cp*). ESI-MS: m/z = 829.04 $[M+H]^+$, 851.03 $[M+Na]^+$. Anal. calcd. (%) for $C_{38}H_{31}F_4RhN_2O_2Ru.1.5H_2O$: C 53.40, H 4.01, N 3.28; found: C 53.45, H 3.99, N 3.33.

Synthesis of [(F2ppy)$_2$Ir(η-Cat)] (3)

Starting with [(F2ppy)$_2$Ir(μ-Cl)]$_2$ (160 mg, 0.16 mmol), AgOTf (185 mg, 0.70 mmol), [Cp*Ru(η-catechol][OTf] (350 mg, 0.7 mmol) and cesium carbonate (470 mg, 1.4 mmol). F2ppy)$_2$Ir(η-Cat)] (**3)** was synthesized according the procedure described above for **2** and isolated as a dark green microcrystalline solid (442 mg) upon recrystallization from THF/hexane. Solvated THF molecules were found in crystals of complex **3**. Yield: 67%.

^{1}H NMR (500 MHz, CD_2Cl_2) : δ 9.05 (d, *J* = 5.8 Hz, 1H, H_2), 8.67 (d, *J* = 5.8 Hz, 1H, $H_{2'}$), 8.26 (d, *J* = 8.4 Hz, 1H, H_5), 8.16 (d, *J* = 8.4 Hz, 1H, $H_{5'}$), 7.88 – 7.84 (m, 1H, H_4), 7.72 – 7.68 (m, 1H, $H_{4'}$), 7.40 – 7.36 (m, 1H, H_3), 7.13 – 7.09 (m, 1H, $H_{3'}$), 6.39 – 6.32 (m, 1H, H_9), 6.34 – 6.28 (m, 1H, $H_{9'}$), 5.66 (dd, *J* = 9.0, 2.3 Hz, 1H, H_{11}), 5.48 (dd, *J* = 9.2, 2.3 Hz, 1H, $H_{11'}$), 4.99 (d, *J* = 5.4 Hz, 1H, H_e), 4.90 (d, *J* = 5.4 Hz, 1H, H_b), 4.47 (t, *J* = 5.4 Hz, 1H, H_c), 4.41 (t, *J* = 5.4 Hz, 1H, H_d), 1.69 (s, 15H, H-Cp*). ^{13}C NMR (125 MHz, CD_2Cl_2) δ 165.3 (d, J_{CF} = 9.4 Hz, C_6), 165.2 (d, J_{CF} = 9.4 Hz, $C_{6'}$), 162.9 (dd, J_{CF} = 254.7; 12.9 Hz, C_{10}), 162.8 (dd, J_{CF} = 254.7; 12.9 Hz, $C_{10'}$), 161.0 (dd, J_{CF} = 259.0; 11.5 Hz, $C_{8'}$), 160.9 (dd, J_{CF} = 259.0; 13.0 Hz, C_8), 153.2 (d, J_{CF} = 7.9 Hz, $C_{12'}$), 152.3 (d, J_{CF} = 7.9 Hz, C_{12}), 149.6 (C_2), 148.3 ($C_{2'}$), 148.2 (C_a), 142.2 (C_f), 137.3 (C_4 and $C_{4'}$), 128.8 (C_7), 122.4 (d, J_{CF} = 19.2 Hz, C_5 and $C_{5'}$), 122.2 (C_3), 121.5 ($C_{3'}$), 114.7 (dd, J_{CF} = 16.5; 2.5 Hz, C_{11}), 113.7 (dd, J_{CF} = 16.5; 2.5 Hz, $C_{11'}$), 96.3 (t, J_{CF} = 27.0 Hz, C_9), 96.2 (t, J_{CF} = 27.0 Hz, $C_{9'}$), 89.5 (Cq-Cp*), 79.1 (C_e), 76.9 (C_d), 76.7 (C_c), 76.3 (C_b), 10.3 (CH_3-Cp*). ESI-MS: m/z = 919.10 $[M+H]^+$, 941.08 $[M+Na]^+$.Anal. calcd. (%) for $C_{38}H_{31}F_4IrN_2O_2Ru.1/4C_4H_4O$: C, 50.33, H, 3.33, N, 3.01 found : C, 50.52, H, 3.72, N, 2.85.

Synthesis of *Λ*-[Ir(F2ppy)2(*L*-pro)] (*Λ*-4). The synthesis of this complex was done following the procedure described by *Ye and coworkers* for *rac*-[(Ir(ppy)$_2$Cl)$_2$]. A mixture of *rac*-[(Ir(F_2ppy)$_2$Cl)$_2$] (178 mg, 0.147 mmol), *L*-pro (50.7 mg, 0.441 mmol), in MeOH (8 mL) was poured into a solution of NaH (14 mg, 0.58 mmol) in MeOH (4ml). The solution was stirred under argon atmosphere at 55 °C for 24 h. The solvent was removed under vacuum, and the resulting material was extracted by 30 mL of CH_2Cl_2. After filtration, the organic phase was then

washed with H_2O (3 x 10 mL) to separate the unreacted *L*-pro. The combined organic extract was dried over $MgSO_4$, filtered, concentrated under reduced pressure and then dried under high vacuum. Yield 74 mg, 41%. ^{1}H NMR spectroscopy in CD_2Cl_2 confirmed the presence of one single diastereomer. ^{1}H-NMR (400 MHz, DMSO-d_6) δ 9.07 (d, J = 5.7 Hz, 1H), 8.70 (d, J = 5.6 Hz, 1H), 8.29 (d, J = 17.7 Hz, 2H), 8.11 (t, J = 7.9 Hz, 1H), 7.59 (dt, J = 21.8, 6.6 Hz, 1H), 6.72 (s, 1H), 6.15 (s, 1H), 5.82 – 5.73 (m, 1H), 5.30 (dd, J = 9.0, 2.5 Hz, 1H), 3.85 (d, J = 6.9 Hz, 1H), 3.35 (s, 8H), 3.35 – 3.26 (m, 1H), 2.27 (s, 1H), 2.02 (s, 1H), 1.75 (s, 1H), 1.41 (s, 2H). ESI-MS: m/z = 688.11 $[M+H]^+$, 710.10 $[M+Na]^+$.

Synthesis of *Δ*-[Ir(F2ppy)2(*D*-pro)] (*Δ*-4). This enantiomeric pure derivative was obtained in 41% yield, (74 mg) by applying the same procedure described above employing instead *D*-pro (50.7 mg, 0,441 mmol.) as starting precursor. The resulting material was rinsed with 15 ml of a saturated KPF_6 solution. ^{1}H NMR examination in CD_2Cl_2 revealed the presence of just one single diastereomer. ^{1}H- NMR (400 MHz, DMSO-d_6) δ 9.07 (d, J = 6.0 Hz, 1H), 8.70 (d, J = 5.7 Hz, 1H), 8.29 (d, J = 18.0 Hz, 2H), 8.11 (t, J = 7.9 Hz, 1H), 7.59 (dt, J = 21.9, 6.3 Hz, 1H), 6.72 (t, J = 11.1 Hz, 1H), 6.15 (d, J = 8.1 Hz, 1H), 5.78 (dd, J = 8.9, 2.4 Hz, 1H), 5.30 (dd, J = 9.0, 2.4 Hz, 1H), 3.90 – 3.82 (m, 1H), 3.49 – 3.30 (m, 3H), 3.32 (s, 1H), 2.47 (s, 1H), 2.26 (s, 1H), 2.02 (s, 1H), 1.78 (d, J = 7.0 Hz, 1H), 1.41 (s, 2H). ESI-MS: m/z = 688.11 $[M+H]^+$, 710.10 $[M+Na]^+$.

Synthesis of *Δ*-[(F2ppy)$_2$Ir(η-Cat)] (*Δ*-**3**). To a yellow solution of complex *Δ*-[Ir(F2ppy)$_2$(D-pro)] (90mg, 0,135mmmol.) in acetonitrile (5 mL) was added aqueous TFA (22ml, 0.3mmol). After stirring for 24 hours, all volatiles were evaporated. After extraction of remaining aqueous phase with CH_2Cl_2 (3x 10 mL), the combined organic phase was dried over $MgSO_4$, filtered and concentrated under vacuum. In an another Schlenk tube, the masked catecholate complex [Cs][η-Cat)] was prepared as described previously using as starting materials [Cp*Ru(η-catechol][OTf] (67 mg, 0.135mmol) and Cs_2CO_3 (90 mg, 0.27 mmol). The yellow solution of the iridium complex in CH_2Cl_2 was added to the [Cs][η-Cat)] in acetone (5mL) and the mixture was stirred

for 1 h. Then the solvent was removed under vacuum, the residue was extracted in CH_2Cl_2 and filtered through celite and dried under vacuum to afford the dark green target compound in microcrystalline solid with 14% yield, 21mg. The ^{1}H-NMR spectrum recorded in CD_2Cl_2 is similar to that of **3**. Also the CD spectrum was recorded.

Synthesis of *Λ*-[(F2ppy)$_2$Ir(η-Cat)] (*Λ*-**3**). This enantiomer was obtained by applying the protocol described for *Δ*-**3**. *Λ*-[(F2ppy)$_2$Ir(η-Cat)] (*Λ*-**3**) was obtained in form of dark green microcrystals in 21% yield, 31mg. The purity of this compound was checked by ^{1}H-NMR spectroscopy in CD_2Cl_2. A CD spectrum of *Λ*-[(F2ppy)$_2$Ir(η-Cat)] (*Λ*-**3**) recorded in CH_2Cl_2 showed mirror image cotton transitions relative to *Δ*-[(F2ppy)$_2$Ir(η-Cat)] (*Δ*-**3**).

X-Ray crystal structure determination. A suitable crystal for x-ray diffraction study was chosen, mounted and placed in a cold nitrogen gas stream. Intensity data was measured with a Bruker Kappa-APEX2 apparatus equipped with a Mo-Kα radiation fine-focus sealed tube. Bruker APEX2 software was used for unit-cell parameters determination, data collection strategy, integration and absorption correction. The WinGX framework was used for solving the structure with SHELXT and refining anisotropically by full-matrix least-squares methods with SHELXL. This structure was sent to the Cambridge Structural Database (deposition number CCDC 1955322) and can be freely retrieved at www.ccdc.cam.ac.uk.

Crystal data for 3. $C_{41}H_{37}F_4IrN_2O_{2.75}Ru$, triclinic P -1, a = 15.0724(4) Å, b = 15.0906(4) Å, c = 17.0709(5) Å, α = 78.598(1)°, β = 74.208(1)°, γ = 74.239(1)°, V = 3563.52(17) Å^3, Z = 4, yellow prism 0.2 × 0.05 × 0.05 mm^3, μ = 4.217 mm^{-1}, min / max transmission = 0.63 / 0.75, T= 200(1) K, λ = 0.71073 Å, θ range = 2.01° to 28.37°, 58770 reflections measured, 17755 independent, R_{int} = 0.0449, completeness = 0.995, 1010 parameters, 105 restraints, final R indices R1 [I>2σ(I)] = 0.0357 and wR2 (all data) = 0.0740, GOF on F^2 = 1.007, largest difference peak / hole = 1.19 / -1.55 e·Å$^-$

ASSOCIATED CONTENT

Supporting Information. X-ray data of **3** and CIF files. ^{1}H DOSY spectra of compounds **2** and **3**. Emission spectra of **2** and **3** performed at ambient temperature and at 77K in MeOH/EtOH(1/4). This material can be freely retrieved at http://pubs.acs.org.

References

1. Flamigni, L.; Barbieri, A.; Sabatini, C.; Ventura, B.; Barigelletti, F. Photochemistry and photophysics of coordination compounds: iridium. *Top. Curr. Chem.* **2007,** 281, 143-203.

2. Yam, V. W. W.; Wong, K. M. C. Luminescent metal complexes of d(6), d(8) and d(10) transition metal centres. *Chem. Commun.* **2011,** 47, 11579-11592.

3. Williams, J. A. G. The coordination chemistry of dipyridylbenzene: N-deficient terpyridine or panacea for brightly luminescent metal complexes? *Chem. Soc. Rev.* **2009,** 38, 1783-1801.

4. Whittle, V. L.; Williams, J. A. G. A New Class of Iridium Complexes Suitable for Stepwise Incorporation into Linear Assemblies: Synthesis, Electrochemistry, and Luminescence. *Inorg. Chem.* **2008,** 47, 6596-6607.

5. You, Y.; Nam, W. Photofunctional triplet excited states of cyclometalated Ir(III) complexes: beyond electroluminescence. *Chem. Soc. Rev.* **2012,** 41, 7061-7084.

6. Gildea, L. F.; Williams, J. A. G. Iridium and platinum complexes for OLEDs. *Woodhead Publ. Ser. Electron. Opt. Mater.* **2013,** 36, 77-113.

7. Hellou, N.; Srebro-Hooper, M.; Favereau, L.; Zinna, F.; Caytan, E.; Toupet, L.; Dorcet, V.; Jean, M.; Vanthuyne, N.; Williams, J. A. G.; Di Bari, L.; Autschbach, J.; Crassous, J. Enantiopure Cycloiridiated Complexes Bearing a Pentahelicenic N-Heterocyclic Carbene and Displaying Long-Lived Circularly Polarized Phosphorescence. *Angew. Chem., Int. Ed.* **2017,** 56, 8236-8239.

8. Brulatti, P.; Gildea, R. J.; Howard, J. A. K.; Fattori, V.; Cocchi, M.; Williams, J. A. G. Luminescent Iridium(III) Complexes with N C N-Coordinated Terdentate Ligands: Dual Tuning of the Emission Energy and Application to Organic Light-Emitting Devices. *Inorg. Chem.* **2012,** 51, 3813-3826.

9. Hierlinger, C.; Trzop, E.; Toupet, L.; Avila, J.; La-Placa, M.-G.; Bolink, H. J.; Guerchais, V.; Zysman-Colman, E. Impact of the use of sterically congested Ir(III)

complexes on the performance of light-emitting electrochemical cells. *Journal of Materials Chemistry C* **2018,** 6, 6385-6397.

10. Szerb, E. I.; Ionescu, A.; Godbert, N.; Yadav, Y. J.; Talarico, A. M.; Ghedini, M. Anionic cyclometallated iridium(III) complexes containing substituted bivalent ortho-hydroquinones. *Inorg. Chem. Comm.* **2013,** 37, 80-83.

11. Morris, C. D.; Spulber, M.; Neuburger, M.; Palivan, C. G.; Constable, E. C.; Housecroft, C. E. Redox cycling of iridium(III) complexes gives versatile materials for photonics applications. *Polyhedron* **2016,** 106, 51-57.

12. Hirani, B.; Li, J.; Djurovich, P. I.; Yousufuddin, M.; Oxgaard, J.; Persson, P.; Wilson, S. R.; Bau, R.; Goddard, W. A., III; Thompson, M. E. Cyclometalated iridium and platinum complexes with noninnocent ligands. *Inorg. Chem.* **2007,** 46, 3865-3875.

13. Lever, A. B. P.; Masui, H.; Metcalfe, R. A.; Stufkens, D. J.; Dodsworth, E. S.; Auburn, P. R. The ground and excited state electronic structures of ruthenium quinones and related species. *Coord. Chem. Rev.* **1993,** 125, 317-31.

14. Ward, M. D.; McCleverty, J. A. Non-innocent behavior in mononuclear and polynuclear complexes: consequences for redox and electronic spectroscopic properties. *J. Chem. Soc., Dalton Trans.* **2002**, 275-288.

15. Grange, C. S.; Meijer, A. J. H. M.; Ward, M. D. Trinuclear ruthenium dioxolene complexes based on the bridging ligand hexahydroxytriphenylene: electrochemistry, spectroscopy, and near-infrared electrochromic behavior associated with a reversible seven-membered redox chain. *Dalton Trans.* **2010,** 39, 200-211.

16. Amouri, H.; Le Bras, J. Taming Reactive Phenol Tautomers and o-Quinone Methides with Transition Metals: A Structure-Reactivity Relationship. *Acc. Chem. Res.* **2002,** 35, 501-510.

17. Le Bras, J.; Amouri, H.; Vaissermann, J. η4-Quinone, η5-semiquinone and η6-hydroquinone complexes of pentamethylcyclopentadienyl iridium. X-ray molecular structure of [Cp*Ir(η4-1,4 benzoquinone)]. *J. Organomet. Chem.* **1998,** 553, 483-485.

18. Moussa, J.; Guyard-Duhayon, C.; Herson, P.; Amouri, H.; Rager, M. N.; Jutand, A. η5-Semiquinone Complexes and the Related η4-Benzoquinone of (Pentamethylcyclopentadienyl)rhodium and -iridium: Synthesis, Structures, Hydrogen Bonding, and Electrochemical Behavior. *Organometallics* **2004,** 23, 6231-6238.

19. Moussa, J.; Lev, D. A.; Boubekeur, K.; Rager, M. N.; Amouri, H. A η4-dithio-para-benzoquinone metal complex. *Angew. Chem., Int. Ed.* **2006,** 45, 3854-3858.

20. Amouri, H.; Moussa, J.; Renfrew, A. K.; Dyson, P. J.; Rager, M. N.; Chamoreau, L.-M. Discovery, structure, and anticancer activity of an iridium complex of diselenobenzoquinone. *Angew. Chem., Int. Ed.* **2010,** 49, 7530-7533.

21. Moussa, J.; Rager, M. N.; Chamoreau, L. M.; Ricard, L.; Amouri, H. Unprecedented π-Bonded Rhodio- and Iridio-o-Benzoquinones as Organometallic Linkers for the Design of Chiral Octahedral Bimetallic Assemblies. *Organometallics* **2009,** 28, 397-404.

22. Moussa, J.; Amouri, H. Supramolecular assemblies based on organometallic quinonoid linkers: a new class of coordination networks. *Angew. Chem., Int. Ed.* **2008,** 47, 1372-1380.

23. Damas, A.; Ventura, B.; Axet, M. R.; Esposti, A. D.; Chamoreau, L.-M.; Barbieri, A.; Amouri, H. Organometallic Quinonoid Linkers: A Versatile Tether for the Design of Panchromatic Ruthenium(II) Heteroleptic Complexes. *Inorg. Chem.* **2010,** 49, 10762-10764.

24. Damas, A.; Ventura, B.; Moussa, J.; Esposti, A. D.; Chamoreau, L.-M.; Barbieri, A.; Amouri, H. Turning on Red and Near-Infrared Phosphorescence in Octahedral Complexes with Metalated Quinones. *Inorg. Chem.* **2012,** 51, 1739-1750.

25. Damas, A.; Gullo, M. P.; Rager, M. N.; Jutand, A.; Barbieri, A.; Amouri, H. Near-infrared room temperature emission from a novel class of Ru(II) heteroleptic complexes with quinonoid organometallic linker. *Chem. Comm.* **2013,** 49, 3796-3798.

26. Moussa, J.; Chamoreau, L.-M.; Esposti, A. D.; Gullo, M. P.; Barbieri, A.; Amouri, H. Tuning Excited States of Bipyridyl Platinum(II) Chromophores with pi-Bonded Catecholate Organometallic Ligands: Synthesis, Structures, TD-DFT Calculations, and Photophysical Properties. *Inorg. Chem.* **2014,** 53, 6624-6633.

27. Sesolis, H.; Moussa, J.; Gontard, G.; Jutand, A.; Gullo, M. P.; Barbieri, A.; Amouri, H. A unique class of neutral cyclometalated platinum(II) complexes with pi-bonded benzenedithiolate: synthesis, molecular structures and tuning of luminescence properties. *Dalton Trans.* **2015,** 44, 2973-2977.

28. Moussa, J.; Loch, A.; Chamoreau, L.-M.; Esposti, A. D.; Bandini, E.; Barbieri, A.; Amouri, H. Luminescent Cyclometalated Platinum Complexes with, pi-Bonded Catecholate Organometallic Ligands. *Inorg. Chem.* **2017,** 56, 2050-2059.

29. Sesolis, H.; Gontard, G.; Jutand, A.; Gullo, M. P.; Bandini, E.; Barbieri, A.; Amouri, H. A Convenient Approach to Luminescent Cyclometalated Platinum(II) Complexes with Organometallic -Bonded Benzenedithiolate. *Eur. J. Inorg. Chem.* **2018**, 3804-3812.

30. Damas, A.; Sesolis, H.; Rager, M. N.; Chamoreau, L. M.; Gullo, M. P.; Barbieri, A.; Amouri, H. Ester-substituted cyclometallated rhodium and iridium coordination assemblies with pi-bonded dioxolene ligand: synthesis, structures and luminescent properties. *Rcs. Adv.* **2014,** 4, 23740-23748.

31. Yao, S. Y.; Ou, Y. L.; Ye, B. H. Asymmetric Synthesis of Enantiomerically Pure Mono- and Binuclear Bis(cyclometalated) Iridium(III) Complexes. *Inorg. Chem.* **2016,** 55, 6018-6026.

32. Yao, S.-Y.; Chen, X.-Y.; Ou, Y.-L.; Ye, B.-H. Chiral Recognition and Dynamic Thermodynamic Resolution of Sulfoxides by Chiral Iridium(III) Complexes. *Inorg. Chem.* **2017,** 56, 878-885.

33. Li, L.-P.; Yao, S.-Y.; Ou, Y.-L.; Wei, L.-Q.; Ye, B.-H. Diastereoselective Synthesis and Photophysical Properties of Bis-Cyclometalated Ir(III) Stereoisomers with Dual Stereocenters. *Organometallics* **2017,** 36, 3257-3265.

34. Ma, J.; Zhang, X.; Huang, X.; Luo, S.; Meggers, E. Preparation of chiral-at-metal catalysts and their use in asymmetric photoredox chemistry. *Nature Protocols* **2018,** 13, 605-632.

35. Zhang, L.; Meggers, E. Steering Asymmetric Lewis Acid Catalysis Exclusively with Octahedral Metal-Centered Chirality. *Acc. Chem. Res.* **2017,** 50, 320-330.

36. Mukherjee, T.; Ghosh, S. K.; Wititsuwannakul, T.; Bhuvanesh, N.; Gladysz, J. A. Chiral-at-Metal Ruthenium Complexes with Guanidinobenzimidazole and Pentaphenylcyclopentadienyl Ligands: Synthesis, Resolution, and Preliminary Screening as Enantioselective Second Coordination Sphere Hydrogen Bond Donor Catalysts. *Organometallics* **2020,** 39, 1163-1175.

37. von Zelewsky, A. *Stereochemistry of Coordination Compounds*. Wiley: Chichester, U.K., 1996; p 254 pp.

38. Collet, A.; Crassous, J.; Dutasta, J. P.; Guy, L. *Molécules Chirales: Stéreochime et Propriétes*. EDP Sciences: 2006.

39. Amouri, H.; Gruselle, M. *Chirality in Transition Metal Chemistry: Molecules, Supramolecular Assemblies and Materials*. Wiley: Chichester, U.K., 2008.

40. Damas, A.; Chamoreau, L. M.; Cooksy, A. L.; Jutand, A.; Amouri, H. pi-Bonded Dithiolene Complexes: Synthesis, Molecular Structures, Electrochemical Behavior, and Density Functional Theory Calculations. *Inorg. Chem.* **2013,** 52, 1409-1417.

41. Quan, L. M.; Stringer, B. D.; Haghighatbin, M. A.; Agugiaro, J.; Barbante, G. J.; Wilson, D. J. D.; Hogan, C. F.; Barnard, P. J. Tuning the electrochemiluminescent properties of iridium complexes of N-heterocyclic carbene ligands. *Dalton Trans.* **2019,** 48, 653-663.

42. Indelli, M. T.; Chiorboli, C.; Scandola, F. In *Photochemistry and Photophysics of Coordination Compounds I*; 2007; Vol. 280, pp 215-255.

43. Montalti, M.; Credi, A.; Prodi, L.; Gandolfi, M. T. *Handbook of Photochemistry*. 3rd ed.; CRC Press: 2006.

44. Maestri, M.; Sandrini, D.; Balzani, V.; Maeder, U.; Vonzelewsky, A. Absorption-Spectra, Electrochemical-Behavior, Luminescence Spectra, and Excited-State Lifetimes of Mixed-Ligand Ortho-Metalated Rhodium(Iii) Complexes. *Inorg. Chem.* **1987,** 26, 1323-1327.

45. Wei, F. F.; Lai, S. L.; Zhao, S. N.; Ng, M.; Chan, M. Y.; Yam, V. W. W.; Wong, K. M. C. Ligand Mediated Luminescence Enhancement in Cyclometalated Rhodium(III) Complexes and Their Applications in Efficient Organic Light-Emitting Devices. *Journal of the American Chemical Society* **2019,** 141, 12863-12871.

46. Soriano-Diaz, I.; Orti, E.; Giussani, A. On the Importance of Ligand-Centered Excited States in the Emission of Cyclometalated Ir(III) Complexes. *Inorg. Chem.* **2021,** 60, 13222-13232.

SYNOPSIS TOC.

Two neutral cyclometalated rhodium and iridium coordination assemblies [$(F2ppy)_2M(\eta\text{-Cat})$], M = Rh, (**2**); M = Ir (**3**) (F2ppy: 2,4-difluorophenylpyridine) displaying a masked *catecholate* (η-Cat) are described. Complexes **2-3** were found to be luminescent and unlike related neutral complexes with free dioxolene ligand with *semiquinone* form, which are non-emissive. At supramolecular level complex **3** self-aggregates via π-π interactions to give a rare 2D Honeycomb structure. Their electrochemical and luminescent properties are presented and discussed.

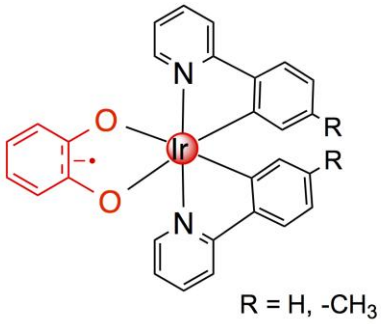

Neutral *semiquinone-form*
non-luminescent

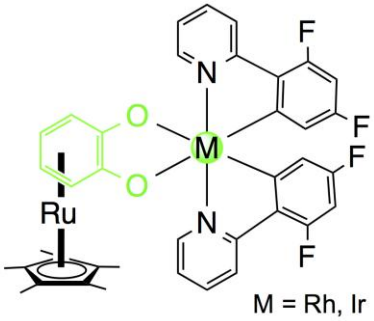

Nuetral *masked-catecholate-form*
luminescent